Variations in CERES-Terra Fluxes and Cloud Properties with SST Anomalies for Low Cloud Regions

Zachary A. Eitzen[1], Kuan-Man Xu[2], and Takmeng Wong[2]

1 – Science Systems and Applications, Inc, Hampton, VA; 2 – Climate Science Branch, NASA Langley Research Center, Hampton, VA

Introduction

The sign and magnitude of the changes in cloud properties for marine boundary-layer cloud regions remains one of the largest sources of uncertainty in the simulation of climate change (e.g., Bony and Dufresne 2005). In this work, we are interested in how cloud and radiative properties vary with SST anomaly in these low cloud regions, based on five years (Mar 2000 - Feb 2005) of CERES (Clouds and the Earth's Radiant Energy System; Wielicki et al. 1996) data. Anomalies in SST and other properties are obtained by calculating the five-year mean for each month, and then subtracting this mean from the observed value. When these anomalies are regressed against one another, a slope of how the property changes per degree of SST is obtained.

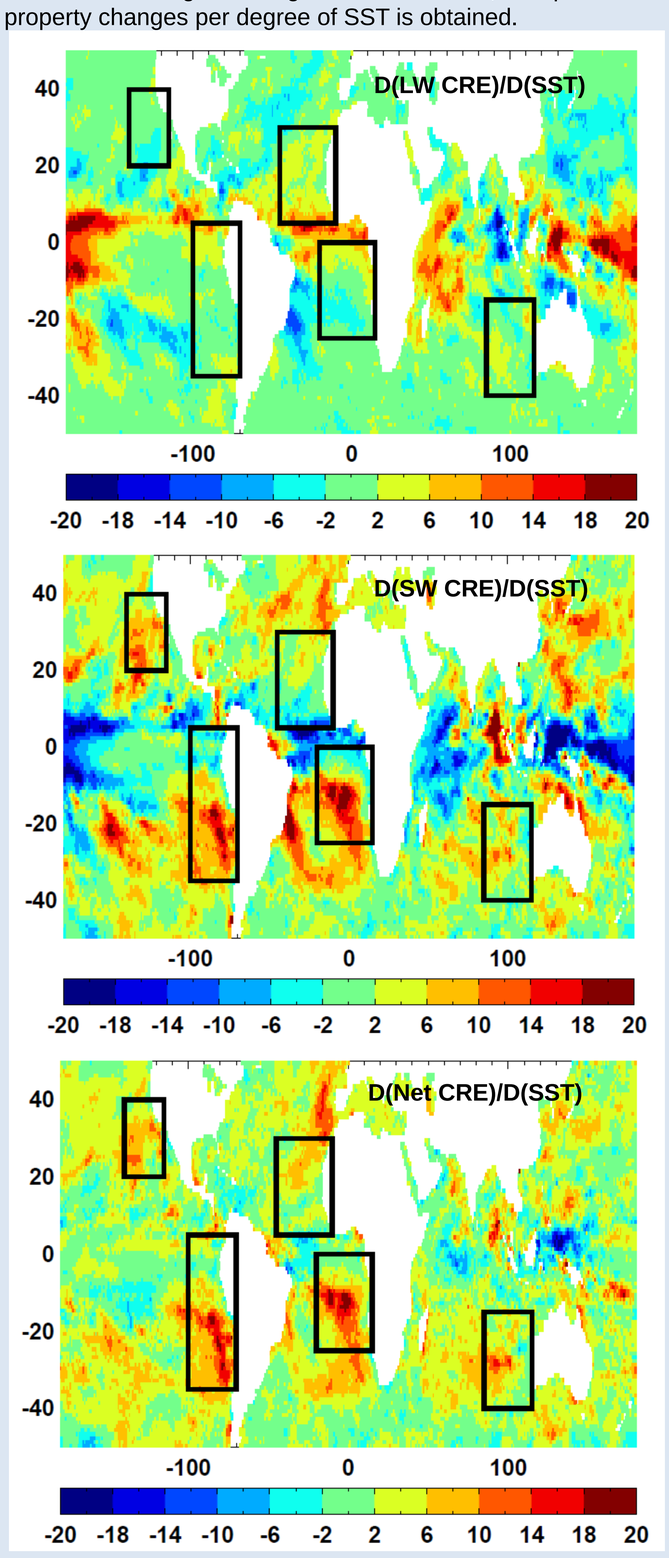

Fig. 1: Change in longwave cloud radiative effect (LW CRE) (top), SW CRE (middle), and net CRE (bottom) per degree of SST. Black boxes indicate the five low-cloud regions defined by Jensen et al. (2008).

Identification of low clouds

Low clouds are isolated by starting from the oceanic portion of the five boxes described by Jensen et al. (2008). Within this subset, only those months and locations which have a five-year mean middle and high cloud fraction of less than 10% are included. There are a total of 94845 observations in this set. The results do not appear to be sensitive to this choice of threshold within the range of 5-15%.

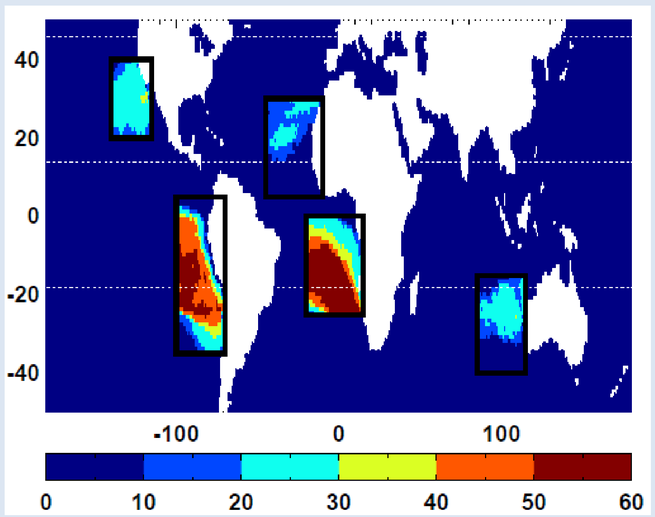

Fig. 2: Number of monthly observations used per 1x1 degree grid cell. Black boxes indicate the five low-cloud regions defined by Jensen et al. (2008).

Thermodynamic and dynamic states

The estimated inversion strength (EIS; Wood and Bretherton 2006) is a measure of lower-tropospheric stability that is positively correlated with low cloud cover. The vertical velocity at 500 hPa (ω_{500}) is frequently used to classify dynamical regimes; here, we use ω_{700} instead. The values of EIS and ω_{700} used here are from ECMWF ERA Interim reanalysis (Uppala et al. 2008). The average anomaly for each ΔEIS- ω_{700} bin is calculated in order to see the effects of changes in thermodynamic and dynamic states on cloud and radiative properties. Most points in the low cloud regions have ω_{700} values corresponding to weak subsidence (10-50 hPa/day), and EIS anomalies between -1.0 and +1.0 K.

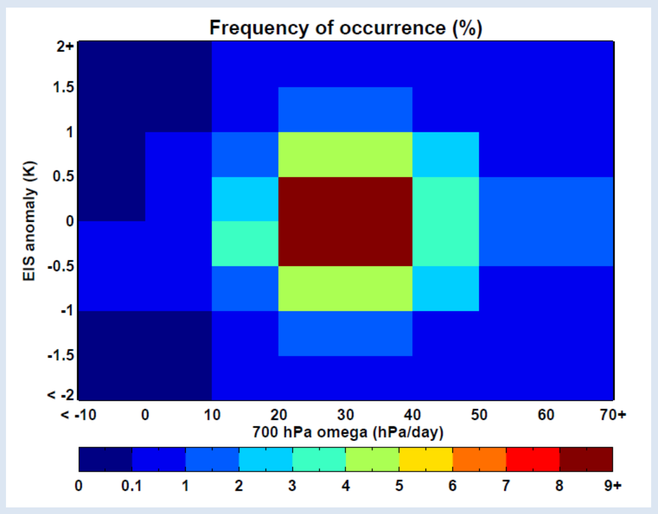

Fig. 3: Frequency of occurrence for each ΔEIS- ω_{700} state associated with the low cloud gridpoints shown in Fig. 2.

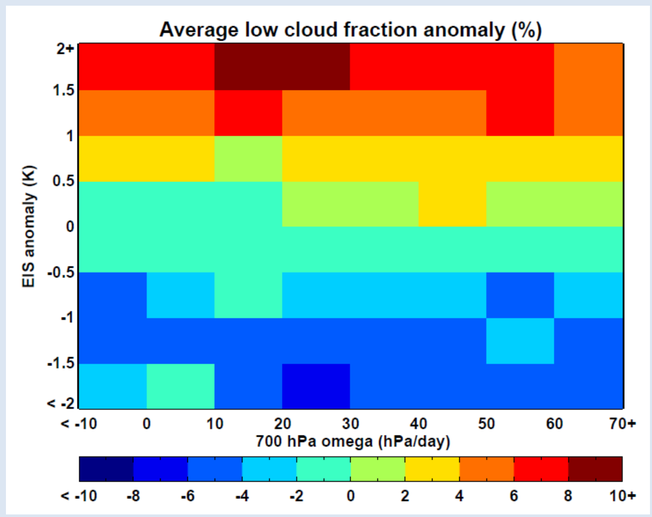

Fig. 4: Average low cloud fraction anomaly for each ΔEIS- ω_{700} state.

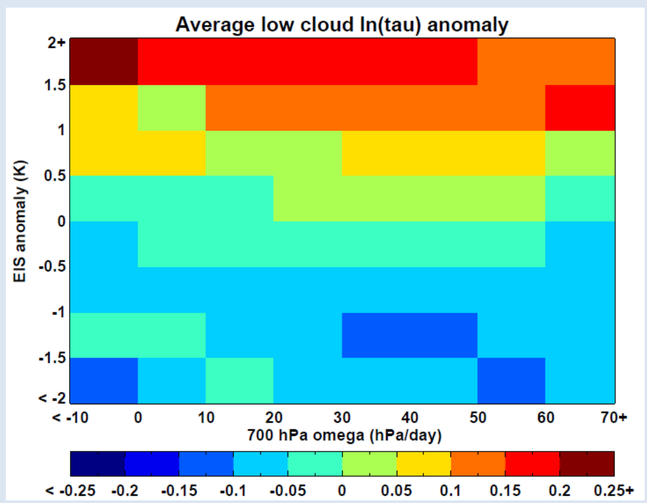

Fig. 5: Average low cloud ln(τ) anomaly for each ΔEIS- ω_{700} state.

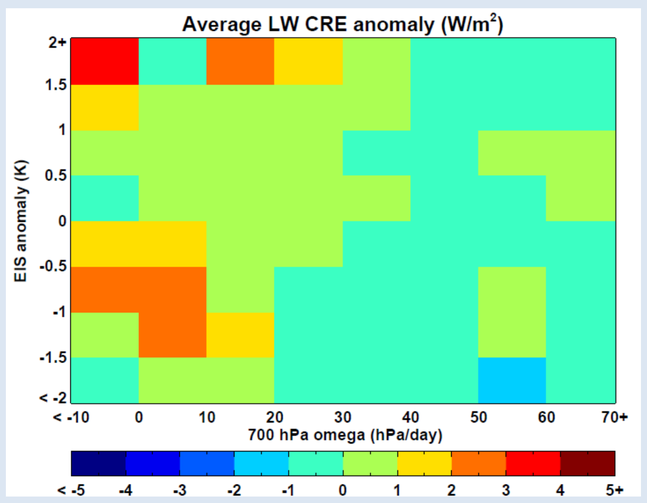

Fig. 6: Average LW CRE anomaly for each ΔEIS- ω_{700} state.

Summary

•Near the ITCZ, clouds become optically thicker (more shortwave cooling) and higher in altitude (more longwave warming) as SST increases, leading to small changes in the net cloud forcing.
•In low cloud regions, cloud cover and optical depth tend to decrease with SST anomaly.
•These changes are associated with a small decrease in longwave warming, but a substantial decrease in shortwave cooling, for a net warming effect.
•The average anomalies of cloud cover and optical depth tend to be strongly positive/negative for positive/negative EIS anomalies throughout the range of ω_{700} regimes present in these regions.
•When these average anomalies are removed, the changes in cloud and radiative properties with SST anomaly decrease in magnitude, but are still of the same sign.

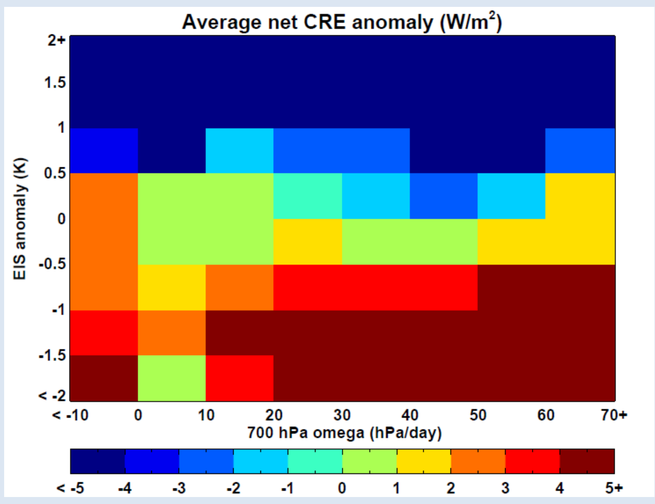

Fig. 7: Average Net CRE anomaly for each ΔEIS- ω_{700} state.

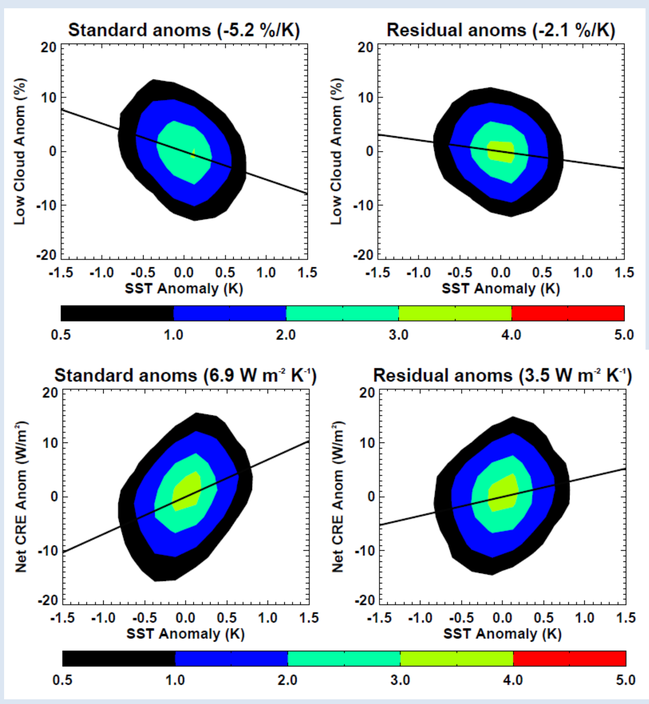

Fig. 8: 2-D histograms of the frequency of occurrence of standard (all) and residual anomalies of low cloud amount (top) and Net CRE versus SST anomaly.

Table 1: Changes in cloud and radiative property anomalies with SST anomaly for low cloud regions shown in Fig. 2. Residual anomalies have the average anomaly for each gridpoint's ΔEIS- ω_{700} bin subtracted from the total anomaly.

Cloud/radiative property	All anomalies	Residual anomalies
Low cloud fraction (% K^{-1})	-5.22	-2.12
Mid/high cloud fraction (% K^{-1})	0.07	-0.26
Low cloud ln(t) (K^{-1})	-0.124	-0.064
LW CRE (W m^{-2} K^{-1})	-0.47	-0.31
SW CRE (W m^{-2} K^{-1})	7.33	3.81
Net CRE (W m^{-2} K^{-1})	6.86	3.50

References

Bony, S., and J.-L. Dufresne, 2005: Marine boundary layer clouds at the heart of tropical cloud feedback uncertainties in climate models. *Geophys. Res. Lett.,* **32,** L20806, doi:10.1029/2005GL023851.

Jensen, M.P., A.M. Vogelmann, W.D. Collins, G.J. Zhang, and E.P. Luke, 2008: Investigation of Regional and Seasonal Variations in Marine Boundary Layer Cloud Properties from MODIS Observations. *J. Climate,* **21,** 4955–4973.

Uppala, S., D. Dee, S. Kobayashi, P. Berrisford, and A. Simmons, 2008: Towards a climate data assimilation system: Status update of ERA-Interim. ECMWF Newsletter No. 115, 12-18.

Wielicki, B. A., B. R. Barkstrom, E. F. Harrison, R. B. Lee III, G. L. Smith, and J. E. Cooper, 1996: Clouds and the Earth's Radiant Energy System (CERES): An Earth Observing System Experiment. *Bull. Amer. Meteor. Soc.,* **77,** 853-868.

Wood, R., and C. S. Bretherton, 2006: On the relationship between stratiform low cloud cover and lower-tropospheric stability. *J. Climate*, **19,** 6425-6432.